Int J Adv Manuf Technol (2017) 93:2975–2984
DOI 10.1007/s00170-017-0715-1

ORIGINAL ARTICLE

Theoretical error compensation when measuring an S-shaped test piece

Liwen Guan[1] · **Jiao Mo**[1] · **Meng Fu**[1] · **Liping Wang**[1]

Received: 16 April 2017 / Accepted: 26 June 2017 / Published online: 11 July 2017

Abstract S-shaped test piece aims to assess the performance of five-axis numerical control (NC) machine tools. When the draft international standard (DIS) was introduced at the 79th ISO/TC39SC2 meeting, it was agreed that this test piece would be included. The S-shaped test piece, however, has undeveloped surfaces, which contribute to theoretical error. Because the test piece is used to assess the performance of machine tools and to conduct error tracing, theoretical error should not be included in the detection results obtained by the coordinate measuring machine (CMM). Therefore, the S-shaped test piece, excluding the influences of theoretical error, is crucial to research. This paper calculates the theoretical error of the S-shaped test piece when processed with the single-point offset (SPO) position method and proposes pre-compensation (PRC) and post-compensation (POC) methods to eliminate the influences of theoretical error. We conducted a theoretical analysis to compare three methods, the two compensation methods and the one uncompensated method, and verified the results through actual experiments. Research from principle and practice demonstrates that both the PRC and POC methods compensated for theoretical error up to 0.01 mm and that PRC is more accurate when considering the difference of approximately ±0.0015 mm.

Keywords Five-axis numerical control machining · Measurement · Theoretical error · Compensation · S-shaped test piece

✉ Liwen Guan
guanlw@mail.tsinghua.edu.cn

[1] Department of Mechanical Engineering, Institute of Manufacturing Engineering, Tsinghua University, Beijing 100084, People's Republic of China

1 Introduction

The five-axis machine tool is presently one of the most versatile tools available, especially in the aeronautics and astronautics industries [1]. These tools have become increasingly popular because of their growing geometric complexity and high-dimensional accuracies. Therefore, the need to improve the performance of five-axis machine tools is significant [2–6]. The Chengdu Aircraft Industrial Group proposed the S-shaped test piece, which integrates many characteristics of aviation parts, for precision measurement [7]. This test piece has been applied in practical testing for many years, and in 2012, it was submitted as an additional sample for standards testing at the 74th ISO meeting [8, 9]. Subsequently, in May 2016, the test piece was added to the draft international standard (DIS) at the 79th ISO/TC39SC2 meeting.

The S-shaped test piece clearly has many advantages in its configuration [10, 11], and such characteristics can be integrated for better detection of accuracy in five-axis numerical control (NC) machine tools. The variegated orientation of the machine tool's ruled surface has higher requirements for the multi-axis linkage ability. Therefore, investigation of the use of the S-shaped test piece and its ability for accuracy measurement holds great theoretical and practical significance. Previous studies [12–15], however, have focused mainly on assessing theory, reconstruction, optimization, and sources of error of the test piece. Theoretical error is well known by researchers, but such influences on measurement and the compensated methods have not been investigated thoroughly.

Although this test piece solves assessment problems associated with five-axis NC machine tools, it also introduces theoretical errors because of the typically undeveloped ruled surface of the S-shaped test piece. Thus, the theoretical error cannot be avoided as long as the radius of the tool is not equal to zero. Hence, when firms use the S-shaped test piece and detect processing results, the theoretical error will affect the results of the analysis. This interference in evaluating the performance of five-axis NC machine tools introduces mistakes in conclusion.

For this reason, theoretical error should be excluded from accuracy detection. Although many flank milling algorithms [16–20] have been proposed, most methods are not practical because of high calculation time or other limitations. Therefore, the traditional single-point offset (SPO) method remains the standard way to conduct flank milling on an undeveloped ruled surface in CAD/CAM software systems [21–23].

When discussing the SPO method, this paper proposes two optional methods to subtract theoretical error: the pre-compensation (PRC) method and the post-compensation (POC) method. By using these methods, the theoretical error of every point on the ruled surface can be eliminated.

This paper is organized as follows: Section 2 introduces the S-shaped test piece and an accurate calculation means for the theoretical method. Section 3 demonstrates the necessity of compensating the theoretical error and proposes the PRC and POC methods. Section 4 explains the problem of the influence of theoretical error in precision measurement through experiments and applies the corresponding resolution methods in actual detection experiment. Section 5 gives the paper's conclusions.

2 Theoretical error of the S-shaped test piece

The three-dimensional model of the S-shaped test piece, with a rectangular base, is shown in Fig. 1. The Cartesian coordinate *O-XYZ* is established (X and Y are datum lines achieved by intersecting the middle plane between plane B1/C1 and plane B2/C2 with plane A). The S-shaped test piece is defined mainly by two S-shaped ruled surfaces, A and B, each of which consists of two quasi-uniform cubic rational B-splines [24], like an S.

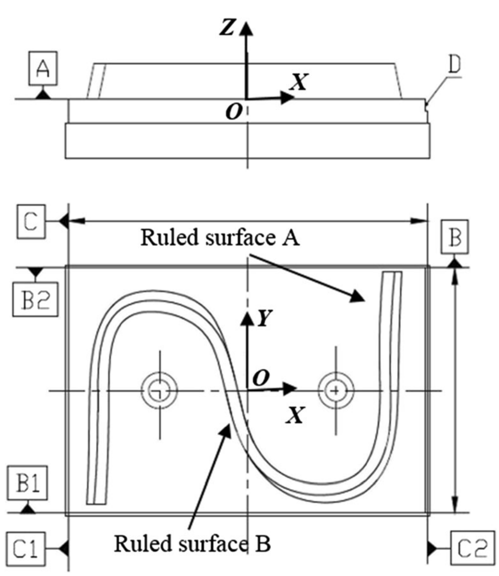

Fig. 1 S-shaped test piece

The main characteristic of the undeveloped ruled surfaces is the twist angle γ, which causes the theoretical error. As shown in Fig. 2, the projections of the upper curve $C_1(u)$ and the lower curve $C_2(u)$ in the view of a ruled line cross each other instead of being coincident, resulting in the twist angle γ between the normal vectors $\boldsymbol{N}_1(u_0)$ and $\boldsymbol{N}_2(u_0)$.

2.1 Calculation method for theoretical error

The calculation method for theoretical error refers to the computation of the theoretical error of the S-shaped test piece under a certain given tool-positioning algorithm, which, in this paper, is the SPO algorithm. The traditional method [22] uses the mathematical formula to solve the theoretical error, which ignores the interplay of adjacent tool positions. To obtain the more accurate theoretical error, we used the minimum distance method [25]. According to this method, many discrete points on the ruled surface are given first, and the minimum distance between each point and the whole range of tool positions is calculated. This minimum distance subtracts the radius of the tool to obtain the theoretical error. The minimum distance method is more direct and easily includes detecting points along the discrete points of the ruled surface, which is beneficial for comparing and analyzing results for accuracy detection. The *MATLAB* program chart of the minimum distance method is as follows (Fig. 3):

The data for the imported tool positions can be the G code data or the position of the tool tip plus the orientation of the vector of the tool axis. If the G code data are imported, they must be transferred to the position of the tool tip and to the orientation of the vector of the tool axis. Considering that each line of G code has defined the values of *X*, *Y*, *Z*, *A*, and *B* (this paper takes AB swing head machine tools as example), we can obtain the position of the tool tip (*X*, *Y*, *Z*) and then calculate the vector of the tool axis by using *A*, *B*. The process of the transfer is related to the coordinate system transformation. We first establish the fixed

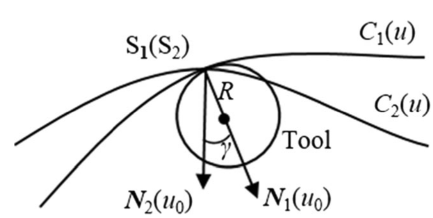

Fig. 2 Projection of curves

Fig. 3 Calculation method for theoretical error

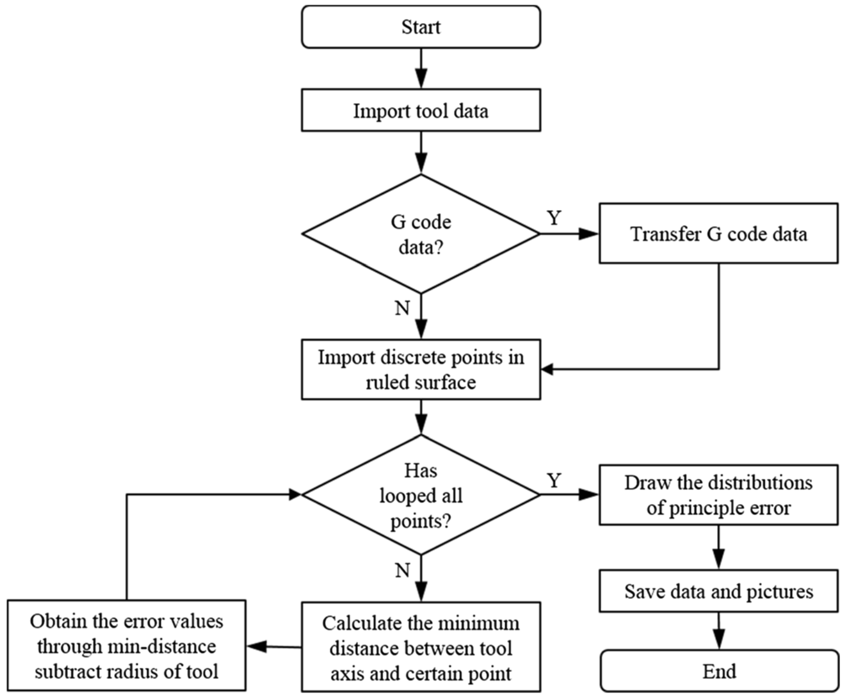

coordinate system $O\text{-}X_0Y_0Z_0$ on the work piece. We next establish the tool coordinate system $o\text{-}xyz$, where the z-axis is upward along the tool axis, and the x-axis and the y-axis are parallel to the X_0-axis and the Y_0-axis, respectively. Finally, the attitude relation between frames $\{o\}$ and $\{O\}$ are described as two continuous rotations with angles B and A around the y-axis and the x-axis (rotated x-axis), respectively. The rotation matrix can be written as follows (symbol c stands for cosine operation, and symbol s stands for sine operation):

$$\mathrm{R}(A,B)=\begin{bmatrix} \mathrm{c}B & \mathrm{s}A\mathrm{s}B & \mathrm{c}A\mathrm{s}B \\ 0 & \mathrm{c}A & -\mathrm{s}A \\ -\mathrm{s}B & \mathrm{c}B\mathrm{s}A & \mathrm{c}A\mathrm{c}B \end{bmatrix}. \quad (1)$$

The vector of the tool axis is expressed as $[0, 0, 1]^\mathrm{T}$ in frame $\{o\}$; thus, this vector is $\boldsymbol{T} = \mathrm{R}\,(A, B)\,[0, 0, 1]^\mathrm{T}$ in frame $\{O\}$.

When solving the distance between a certain point and the tool axis, we use the vector method to obtain this value rapidly. The theory of the vector method is shown in Fig. 4, where

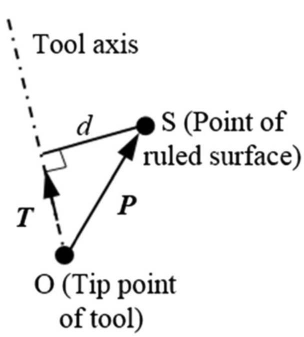

Fig. 4 Theory of vector method

$\boldsymbol{T}$ is the unit vector of the tool axis, $\boldsymbol{P}$ is the vector from point O to point S, and d is the distance from S to the tool axis.

The plus or minus of $(\boldsymbol{P}\cdot\boldsymbol{T})$ is important because the angle between the two vectors $\boldsymbol{P}$ and $\boldsymbol{T}$ has the possibility to be greater than 90°. If $(\boldsymbol{P}\cdot\boldsymbol{T}) > 0$, then $d = (||\boldsymbol{P}||^2 - (\boldsymbol{P}\cdot\boldsymbol{T})^2)^{1/2}$, and otherwise, $d = ||\boldsymbol{P}||$. Finally, traversal operators can give the minimum distance, and the theoretical error is equal to the minimum distance subtract the tool radius R.

2.2 Distribution of theoretical error

Figure 5 presents the distribution of theoretical error of the S-shaped test piece processed using the SPO method.

The general features and trends of the distributions are discussed as follows.

(1) For surface A, relatively larger error values appear in three areas where X is approximately equal to 40, 140, and 250 (the homologous arc lengths are about 130, 270, and 480, respectively). And for surface B, relatively larger error values appear in three areas where X is approximately equal to 40, 120, and 260 (the homologous arc lengths are about 130, 240, and 530, respectively).

(2) The largest theoretical error for surface A is about 25 μm, while for surface B, it appears to be 20 μm. And the theoretical error in two surfaces is less than 10 μm for most areas.

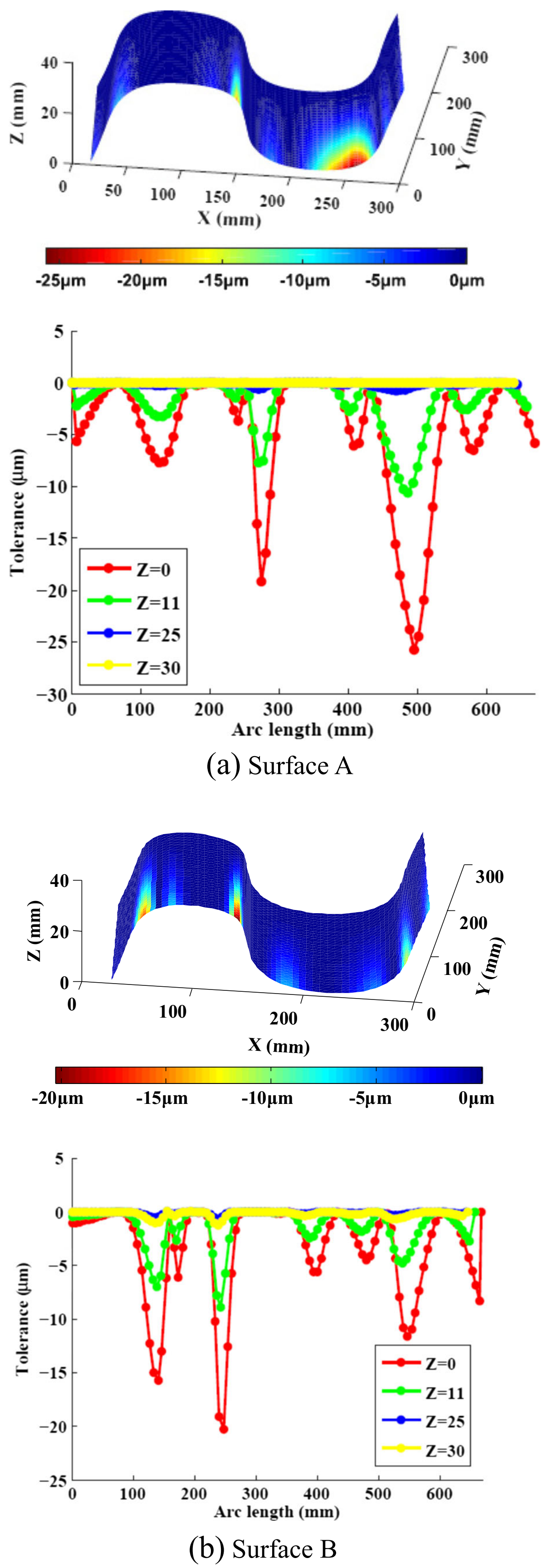

Fig. 5 Distributions of theoretical error. **a** Surface A. **b** Surface B

3 Theoretical error compensation of accuracy detection

3.1 Reasons for compensation

The measurement results of the processing error are expected to effectively reflect the performance of the machine tool. The main characteristic of the S-shaped test piece, however (i.e., the inconsistent size and direction of its curvatures), introduces an irregular theoretical error. The S-shaped test piece is applied to evaluate the five-axis NC machine tools by using its sharp changes for the tool axis vector when flank milling cylindrical tools. The non-uniform changes will lead directly to severe fluctuations in the processing of milling force, causing tool and part vibration, which disrupts machine stability [12]. Therefore, the theoretical error should not be included in accuracy detection because it is incapable of assessing the performance of machine tools. In a special case, suppose that the undercut error caused by the machine tool, plus the overcut error induced by position algorithm, equals 0. This process result would indicate absolute accuracy. Nevertheless, the performance of the machine tool is affected adversely when compensating for this theoretical error.

According to the present DIS, the recommended measurement points are located on the planes $Z = 11$ and $Z = 25$, for which the theoretical error is approximately less than 5 μm. Because the widely recognized standard requires an allowable range of final error from −50 to +50 μm, the theoretical error seems to be negligible. It is obvious, however, that the theoretical error has significant effects when the S-shaped test piece is considered to be nearly unqualified or qualified for use. Assuming that the maximum overcut error equals a value between −50 and −55 μm, the test piece instead might be qualified when considering the theoretical error. The maximum undercut error, between 45 and 50 μm, in turn, might indicate that the test piece is unqualified. Additionally, if the S-shaped test piece is

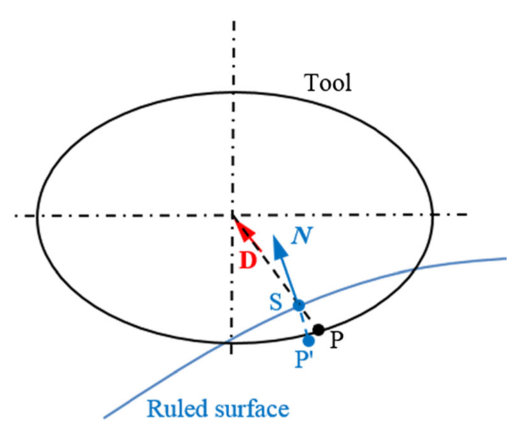

Fig. 6 Diagrammatic sketch of PRC and POC

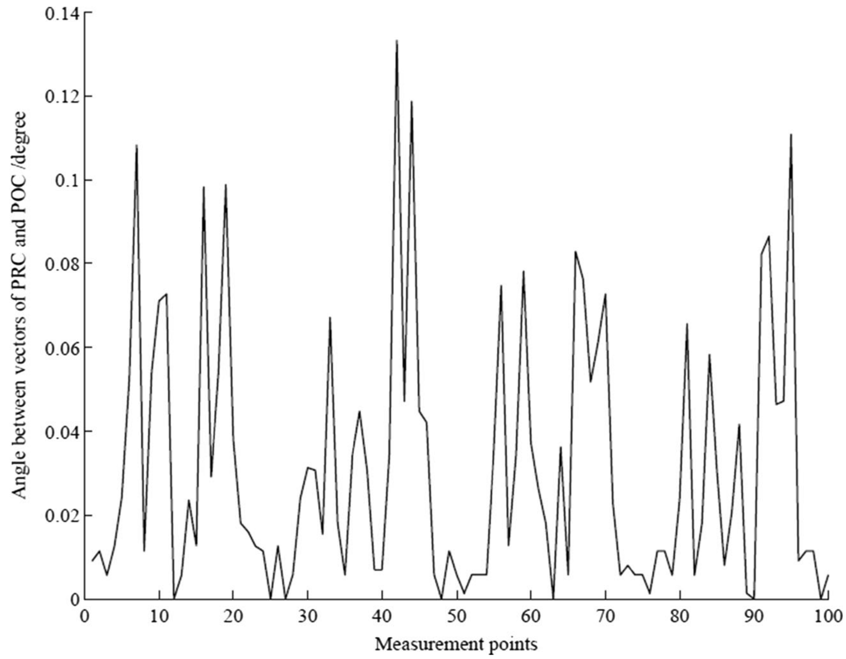

Fig. 7 Angle between vectors of the PRC and the POC methods

considered to be unqualified, it would be necessary to find the causes, which require the accurate distribution of machining error. So the accurate distribution of machining error requires not only the measurement points located on the planes Z = 11 and Z = 25, which would include the maximum theoretical error 25 μm. From this perspective, the compensation of theoretical error is more reasonable. Furthermore, the compensation methods are convenient and may be conducted quickly (demonstrated in Section 3.2) without additional cost.

3.2 PRC and POC methods

Resolution strategies require a decrease in the theoretical error, and therefore, this paper proposes two methods to solve this problem. One, the PRC method, offsets the theoretical error before deciding on the data of the measurement points; and the second, the POC method, offsets the theoretical error after accuracy detection. On the basis of the PRC method, the measurement points are calculated by tool position. In reference to Fig. 4, the vector ***D*** and point P (S – theoretical error value ×

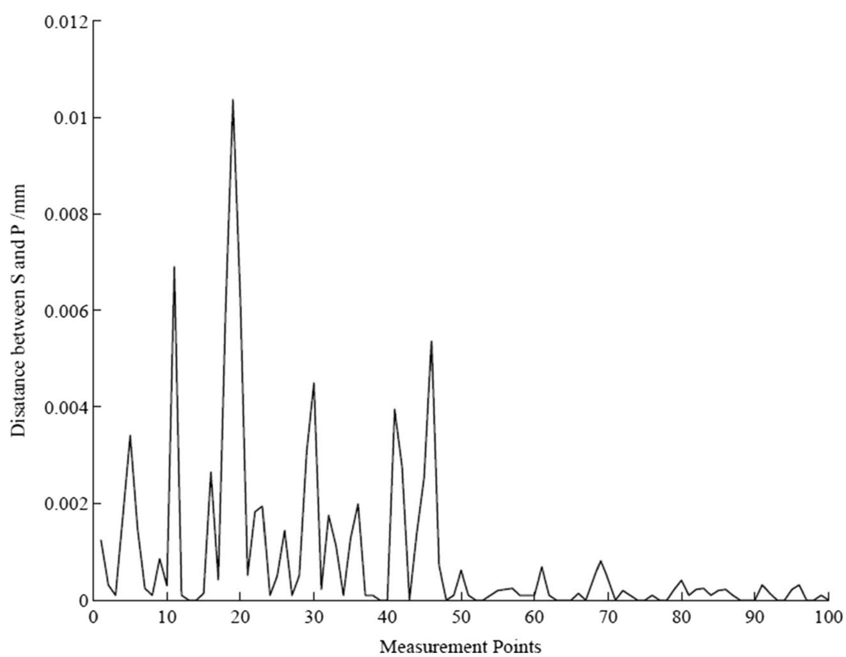

Fig. 8 Distance between S and P

D) are the exact data of the measurement points, where ***D*** is the unit vector from S to the tool axis. For the POC method, however, it is not necessary to first correct the measurement points constructed by point S and normal vector ***N*** of the ruled surface. Instead, the theoretical error is subtracted after detection, which is equivalent to measure P′. The measurement points given by DIS, POC, and PRC are demonstrated in the Appendix.

Theoretically, the PRC method is more accurate because the test points and their normal vector must have changed once the tool position was confirmed. As shown in Fig. 6, S is the original test point, and P is the actual position of the machined S. The vector ***D*** and point P can be obtained by the method mentioned in Section 2.1. And the vector ***N*** and point S can be calculated from the definition of the S-shaped test piece.

As presented in Fig. 7, however, the angle between the vectors of the PRC and the POC methods is nearly 0, making the POC method efficient as well. Conversely, this result also proves that the PRC method is more precise than the POC method. In addition, although the distance between points S and P is not equal to 0, as shown in Fig. 8, it is also the theoretical error that would be subtracted after detection, according to the POC method. The maximum value of the

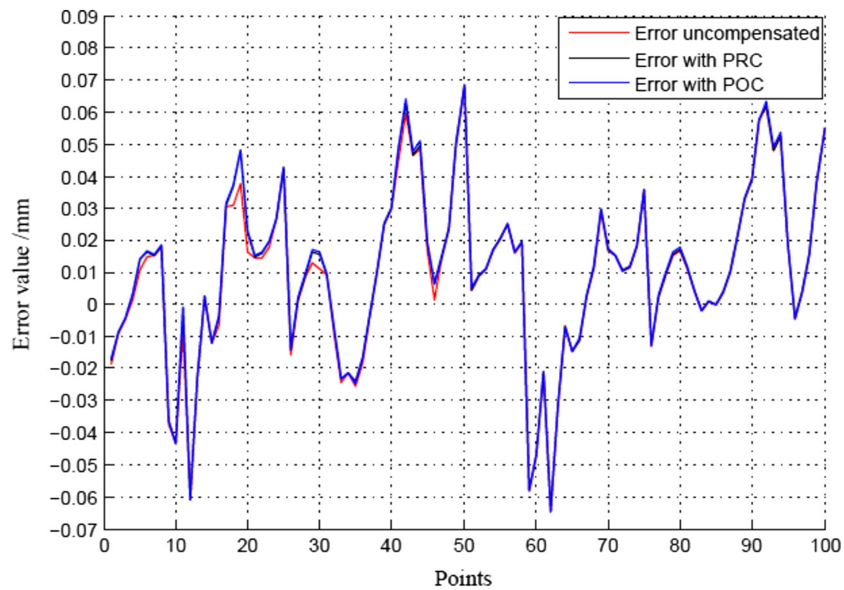

(a) Test Piece 1

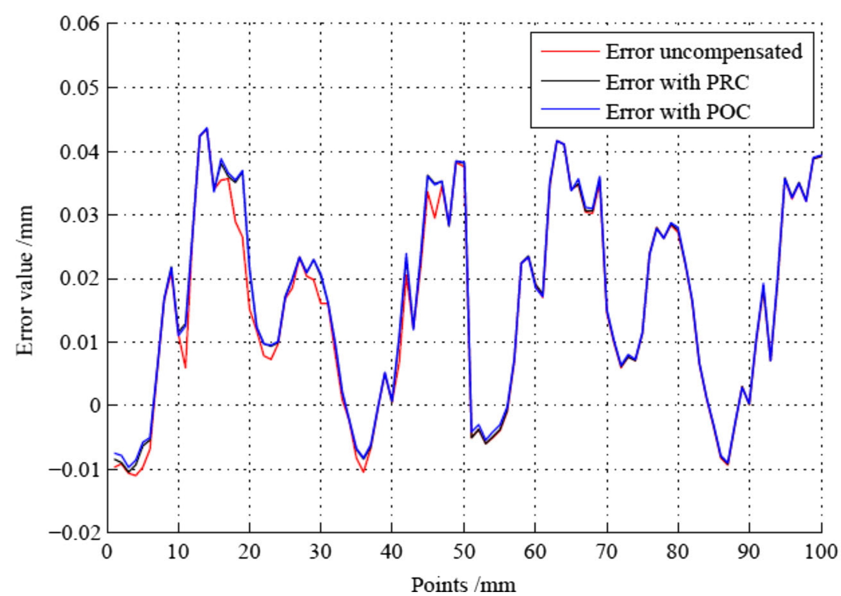

(b) Test Piece 2

Fig. 9 Error results of the experiments. **a** Test piece 1. **b** Test piece 2

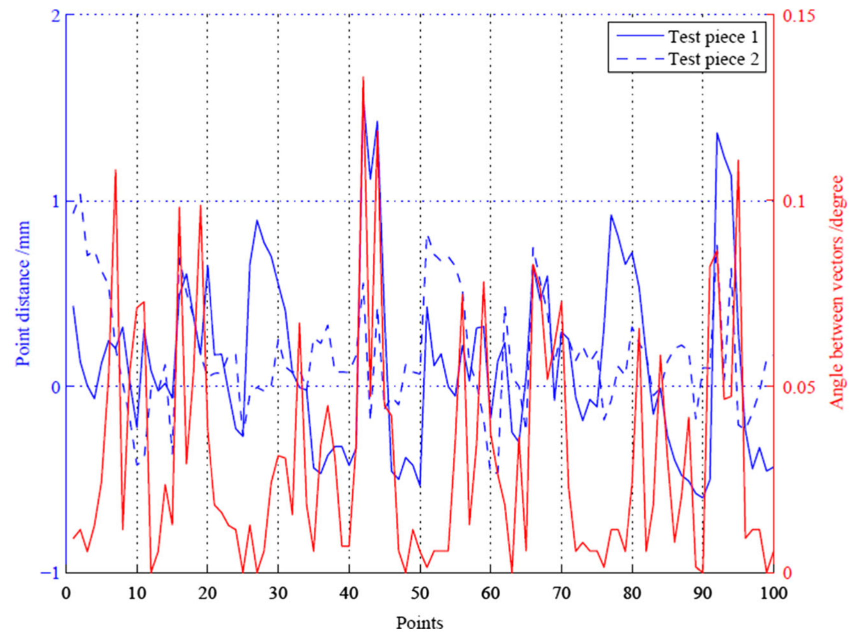

Fig. 10 Differences of results between PRC and POC

distance between S and P is approximately 0.01 mm, which would be the maximum value difference between the uncompensated method and the POC method. In other words, the curve of the distance between S and P is just the difference between the uncompensated method and the POC method. Therefore, the only slight difference between the two compensated methods is from the vectors, indicating that the POC and PRC methods would obtain similar results and that any dissimilarity should relate to the angle between their vectors.

4 Experiments

We machined two S-shaped test pieces with the SPO position method at the machining center VMC35120U of the Shenyang No. 1 Machine Tool Factory. These test pieces were then detected using a coordinate measuring machine. The measurement points used are demonstrated in the PRC and POC methods and are shown in the Appendix.

The error results of the experiments are shown in Fig. 9a (test piece 1) and b (test piece 2). From the pictures and the judgment standard discussed earlier, test piece 1 is considered to be unqualified, and test piece 2 is considered to be qualified. Despite these qualifications, significant differences are apparent between uncompensated error and compensated error. The biggest difference is approximately 0.01 mm at point 19 of test piece 1, and most of the differences are approximately 0.005 mm, in accordance with the theoretical analysis in Fig. 8. Although it seems to make no different in most situations, the error value near the critical point, such as at the 13th point in Fig. 8, is likely to influence the decision to qualify the test piece or not. In addition, the uncompensated error might exercise an influence on the analysis of the source of error. Therefore, considering the low cost and convenience of the method, it actually is necessary to compensate the measurement.

The specific differences between the PRC and the POC could be obtained from further study. By subtracting the POC from the PRC, Fig. 10 investigates the calculation results, along with the angle between their vectors. No obvious relationship exists between the qualified test piece and the unqualified test piece. The consequences demonstrate that the differences in the results between PRC and POC are as low as anticipated, which in most cases, are less than 0.001 mm. Therefore, a shortage does not exist to the extent that the POC method should be abandoned. Certainly, if the search for sources of error must be especially precise, it is best to use the PRC method. In addition, the tendency of the differences between the PRC and POC is related to the angle of their vectors, which is particularly apparent from the 40th point to the 50th point.

5 Conclusions

Considering the important application of the S-shaped test piece, this paper investigates the detection error caused by DIS measurement points, which is beneficial to tracking errors and making qualified judgments. After explaining why it is necessary to eliminate this error, two methods, PRC and POC, were proposed to prevent the error. Finally, two S-shaped test pieces were machined to verify the theory that both the PRC and the POC methods efficiently eliminate measurement error. The experiment also concludes that the PRC and the POC methods would decrease error by 0.01 mm. In addition, the PRC method is more suitable than the POC method when considering the difference of 0.0015 mm. Furthermore, using the PRC method to substitute the DIS measurement points is the best choice. On the basis of the application of PRC, further research can be conducted to better identify sources of machining error.

Acknowledgments This research was financially supported by the Major National S&T Program (No. 2014ZX04014-031) and by the National Natural Science Foundation of China (Grant No. 51675301).

Appendix

Measurement points according to DIS, POC, and PRC are presented in Tables 1 and 2.

Table 1 Measurements points in DIS and POC

X	*Y*	*Z*	*I*	*J*	*K*
−133.3897	−70.2753	11	−0.9744	0.0421	0.2207
−132.6081	−45.0234	11	−0.9717	0.0189	0.2356
−132.3142	−19.7602	11	−0.9714	0.0070	0.2374
−131.9212	5.5007	11	−0.9742	0.0333	0.2232
−129.8374	30.6656	11	−0.9694	0.1447	0.1984
−123.3116	54.9968	11	−0.8986	0.3961	0.1888
−107.508	74.1908	11	−0.5044	0.8307	0.2355
−83.3703	80.7191	11	−0.0422	0.9660	0.2552
−58.3815	77.7799	11	0.2633	0.9301	0.2559
−36.2769	66.0187	11	0.6547	0.7253	0.2129
−21.9793	45.4131	11	0.9100	0.4098	0.0630
−13.9012	21.5053	11	0.9673	0.2537	0.0015
−7.7502	−2.9991	11	0.9701	0.2425	0.0000
−1.4211	−27.4554	11	0.9554	0.2952	0.0005
8.8422	−50.4697	11	0.8530	0.5218	−0.0055
25.3731	−69.3914	11	0.6113	0.7884	−0.0687
48.0421	−80.0882	11	0.2263	0.9615	−0.1561
73.139	−81.4644	11	−0.1233	0.9737	−0.1914
96.4168	−72.4682	11	−0.6077	0.7633	−0.2192
109.8441	−51.4944	11	−0.9312	0.3059	−0.1982
114.5502	−26.7236	11	−0.9812	0.0938	−0.1685
115.7953	−1.4957	11	−0.9845	0.0179	−0.1743
116.0294	23.7679	11	−0.9793	0.0081	−0.2021
116.4382	49.0294	11	−0.9755	0.0253	−0.2187
117.364	74.2764	11	−0.9753	0.0461	−0.2160
127.2761	74.3317	11	0.9736	−0.0489	0.2230
126.2772	49.1371	11	0.9713	−0.0284	0.2361
125.7725	23.9276	11	0.9725	−0.0118	0.2326
125.5188	−1.286	11	0.9774	−0.0131	0.2111
124.559	−26.4778	11	0.9804	−0.0799	0.1800
120.0981	−51.2424	11	0.9401	−0.2919	0.1761
108.4583	−73.4205	11	0.7469	−0.6294	0.2142
88.0226	−87.6978	11	0.3387	−0.9119	0.2318
63.2639	−91.6433	11	−0.0172	−0.9789	0.2035
38.5629	−87.1719	11	−0.3374	−0.9308	0.1410

Table 1 (continued)

X	*Y*	*Z*	*I*	*J*	*K*
17.042	−74.3206	11	−0.6584	−0.7510	0.0502
0.8217	−55.1247	11	−0.8432	−0.5375	0.0032
−10.1928	−32.5015	11	−0.9416	−0.3368	−0.0013
−16.945	−8.2201	11	−0.9701	−0.2425	0.0000
−23.0605	16.2419	11	−0.9701	−0.2425	0.0000
−30.6259	40.2603	11	−0.9141	−0.4041	−0.0339
−45.8106	60.0031	11	−0.5826	−0.7941	−0.1732
−68.9007	69.6409	11	−0.1943	−0.9535	−0.2304
−93.8988	69.5839	11	0.2507	−0.9397	−0.2327
−113.1265	54.4177	11	0.8577	−0.4840	−0.1734
−120.5185	30.4534	11	0.9711	−0.1452	−0.1896
−122.3174	5.3198	11	0.9767	−0.0222	−0.2134
−122.609	−19.8931	11	0.9756	−0.0088	−0.2196
−122.9725	−45.1052	11	0.9762	−0.0207	−0.2157
−123.699	−70.3092	11	0.9777	−0.0357	−0.2070
−130.2508	−70.8527	25	−0.9739	0.0545	0.2201
−129.2423	−46.1643	25	−0.9716	0.0253	0.2352
−128.9006	−21.4568	25	−0.9713	0.0042	0.2377
−128.762	3.2527	25	−0.9744	0.0160	0.2244
−127.3413	27.9113	25	−0.9732	0.1151	0.1991
−121.7153	51.8975	25	−0.9099	0.3703	0.1871
−106.5213	70.8216	25	−0.5002	0.8332	0.2358
−82.8697	77.0408	25	−0.0357	0.9662	0.2552
−58.4602	73.9478	25	0.2752	0.9269	0.2554
−36.8307	62.3857	25	0.6350	0.7410	0.2185
−21.8863	42.9091	25	0.8887	0.4516	0.0795
−13.4567	19.7313	25	0.9669	0.2552	0.0016
−7.4411	−4.2354	25	0.9701	0.2425	0.0000
−1.2141	−28.1447	25	0.9541	0.2995	0.0006
9.0048	−50.5643	25	0.8431	0.5377	−0.0071
25.8296	−68.4381	25	0.5691	0.8184	−0.0794
48.4746	−77.8874	25	0.1983	0.9670	−0.1599
73.0493	−78.7292	25	−0.1426	0.9713	−0.1903
95.4607	−69.1671	25	−0.6479	0.7297	−0.2187
107.9623	−48.2013	25	−0.9355	0.2953	−0.1941
112.4126	−23.9435	25	−0.9820	0.0876	−0.1674
113.3236	0.7416	25	−0.9843	0.0001	−0.1762
113.1314	25.4509	25	−0.9790	−0.0053	−0.2036
113.3254	50.1599	25	−0.9755	0.0226	−0.2190
114.2947	74.8495	25	−0.9750	0.0536	−0.2157
124.1006	74.8744	25	0.9729	−0.0614	0.2227
122.9072	50.2047	25	0.9712	−0.0325	0.2361
122.437	25.5105	25	0.9725	−0.0054	0.2327
122.5035	0.8112	25	0.9775	0.0056	0.2111
122.1729	−23.8829	25	0.9825	−0.0519	0.1791
118.3982	−48.2347	25	0.9452	−0.2757	0.1748
107.2569	−70.0869	25	0.7532	−0.6225	0.2127
87.4266	−84.3549	25	0.3549	−0.9057	0.2317
63.2523	−88.7096	25	0.0066	−0.9784	0.2066

Table 1 (continued)

X	*Y*	*Z*	*I*	*J*	*K*
38.9149	−85.1147	25	−0.2968	−0.9430	0.1503
17.2732	−73.5215	25	−0.6272	−0.7766	0.0584
0.9045	−55.1578	25	−0.8362	−0.5484	0.0042
−10.011	−33.064	25	−0.9406	−0.3396	−0.0014
−16.6764	−9.2943	25	−0.9701	−0.2425	0.0000
−22.667	14.668	25	−0.9701	−0.2425	0.0000
−30.2159	38.1402	25	−0.9042	−0.4254	−0.0385
−45.7868	56.9179	25	−0.5601	−0.8091	−0.1782
−68.5053	66.1778	25	−0.1946	−0.9535	−0.2303
−93.0125	66.347	25	0.2304	−0.9447	−0.2335
−111.8368	51.6556	25	0.8731	−0.4563	−0.1717
−118.1152	27.9078	25	0.9755	−0.1095	−0.1910
−119.2883	3.2467	25	0.9767	−0.0113	−0.2142
−119.473	−21.4523	25	0.9756	−0.0096	−0.2195
−119.9057	−46.1475	25	0.9762	−0.0253	−0.2154
−120.7568	−70.832	25	0.9775	−0.0418	−0.2068

Table 2 Measurements points in PRC

X	*Y*	*Z*	*I*	*J*	*K*
−133.3885	−70.2754	10.9997	−0.9745	0.0420	0.2206
−132.6078	−45.0234	10.9999	−0.9717	0.0191	0.2356
−132.3141	−19.7602	11.0000	−0.9714	0.0070	0.2373
−131.9195	5.5006	10.9996	−0.9742	0.0334	0.2230
−129.8341	30.6651	10.9993	−0.9694	0.1450	0.1981
−123.3103	54.9962	10.9997	−0.8990	0.3953	0.1886
−107.5079	74.1906	10.9999	−0.5028	0.8317	0.2356
−83.3703	80.719	11.0000	−0.0420	0.9660	0.2552
−58.3817	77.7791	10.9998	0.2624	0.9304	0.2559
−36.2771	66.0185	10.9999	0.6556	0.7245	0.2126
−21.9856	45.4103	10.9996	0.9104	0.4090	0.0621
−13.9013	21.5053	11.0000	0.9673	0.2537	0.0015
−7.7502	−2.9991	11.0000	0.9701	0.2426	0.0000
−1.4211	−27.4554	11.0000	0.9553	0.2956	0.0005
8.8421	−50.4698	11.0000	0.8529	0.5220	−0.0055
25.3715	−69.3935	11.0002	0.6100	0.7894	−0.0692
48.042	−80.0886	11.0001	0.2268	0.9614	−0.1561
73.1397	−81.4703	11.0012	−0.1239	0.9735	−0.1921
96.4231	−72.4761	11.0023	−0.6064	0.7641	−0.2200
109.8499	−51.4963	11.0012	−0.9310	0.3061	−0.1988
114.5507	−26.7236	11.0001	−0.9812	0.0935	−0.1686
115.7971	−1.4957	11.0003	−0.9845	0.0181	−0.1745
116.0313	23.7679	11.0004	−0.9793	0.0082	−0.2023
116.4383	49.0294	11.0000	−0.9755	0.0255	−0.2187
117.3645	74.2764	11.0001	−0.9753	0.0461	−0.2160
127.2747	74.3318	10.9997	0.9736	−0.0487	0.2229
126.2771	49.1371	11.0000	0.9713	−0.0284	0.2361
125.772	23.9276	10.9999	0.9725	−0.0119	0.2326
125.5158	−1.286	10.9993	0.9774	−0.0134	0.2108
124.5546	−26.4774	10.9992	0.9805	−0.0801	0.1795
120.0979	−51.2423	11.0000	0.9399	−0.2924	0.1761
108.457	−73.4194	10.9996	0.7469	−0.6296	0.2140
88.0222	−87.6968	10.9997	0.3398	−0.9115	0.2318
63.2639	−91.6432	11.0000	−0.0175	−0.9789	0.2034
38.5633	−87.1707	10.9998	−0.3374	−0.9308	0.1409

Table 2 (continued)

X	*Y*	*Z*	*I*	*J*	*K*
17.0433	−74.3191	10.9999	−0.6588	−0.7506	0.0500
0.8218	−55.1247	11.0000	−0.8437	−0.5369	0.0031
−10.1927	−32.5015	11.0000	−0.9418	−0.3363	−0.0013
−16.945	−8.2201	11.0000	−0.9702	−0.2424	0.0000
−23.0605	16.2419	11.0000	−0.9702	−0.2424	0.0000
−30.6223	40.2619	11.0001	−0.9139	−0.4045	−0.0343
−45.809	60.0053	11.0005	−0.5807	−0.7953	−0.1738
−68.9007	69.6409	11.0000	−0.1935	−0.9537	−0.2304
−93.8991	69.5852	11.0003	0.2487	−0.9402	−0.2329
−113.1287	54.4189	11.0004	0.8573	−0.4846	−0.1737
−120.5237	30.4542	11.0010	0.9709	−0.1457	−0.1901
−122.3181	5.3198	11.0001	0.9767	−0.0223	−0.2134
−122.609	−19.8931	11.0000	0.9756	−0.0088	−0.2196
−122.9726	−45.1052	11.0000	0.9762	−0.0209	−0.2157
−123.6996	−70.3092	11.0001	0.9777	−0.0357	−0.2071
−130.2507	−70.8527	25.0000	−0.9740	0.0545	0.2201
−129.2423	−46.1643	25.0000	−0.9716	0.0254	0.2352
−128.9006	−21.4568	25.0000	−0.9713	0.0043	0.2377
−128.7619	3.2527	25.0000	−0.9744	0.0161	0.2244
−127.3411	27.9113	25.0000	−0.9731	0.1157	0.1990
−121.7151	51.8974	25.0000	−0.9094	0.3715	0.1872
−106.5212	70.8214	24.9999	−0.5004	0.8331	0.2358
−82.8697	77.0407	25.0000	−0.0351	0.9662	0.2552
−58.4602	73.9477	25.0000	0.2765	0.9265	0.2553
−36.8307	62.3856	25.0000	0.6345	0.7414	0.2186
−21.8869	42.9088	24.9999	0.8885	0.4520	0.0794
−13.4568	19.7313	25.0000	0.9670	0.2549	0.0016
−7.4411	−4.2354	25.0000	0.9701	0.2425	0.0000
−1.2141	−28.1447	25.0000	0.9539	0.3001	0.0006
9.0048	−50.5643	25.0000	0.8431	0.5377	−0.0072
25.8295	−68.4382	25.0000	0.5703	0.8176	−0.0793
48.4746	−77.8874	25.0000	0.1996	0.9668	−0.1597
73.0494	−78.7296	25.0001	−0.1417	0.9714	−0.1903
95.4612	−69.1677	25.0002	−0.6486	0.7290	−0.2191
107.9627	−48.2014	25.0001	−0.9351	0.2965	−0.1942
112.4126	−23.9435	25.0000	−0.9820	0.0880	−0.1674
113.3238	0.7416	25.0000	−0.9843	0.0001	−0.1763
113.1315	25.4509	25.0000	−0.9790	−0.0054	−0.2037
113.3254	50.1599	25.0000	−0.9755	0.0225	−0.2190
114.2947	74.8495	25.0000	−0.9750	0.0535	−0.2157
124.1005	74.8744	25.0000	0.9730	−0.0614	0.2227
122.9072	50.2047	25.0000	0.9712	−0.0327	0.2361
122.437	25.5105	25.0000	0.9725	−0.0056	0.2327
122.5033	0.8112	24.9999	0.9775	0.0056	0.2110
122.1725	−23.8829	24.9999	0.9825	−0.0523	0.1790
118.3981	−48.2347	25.0000	0.9449	−0.2768	0.1749
107.2567	−70.0868	25.0000	0.7532	−0.6225	0.2126
87.4265	−84.3547	24.9999	0.3552	−0.9056	0.2317
63.2523	−88.7095	25.0000	0.0076	−0.9784	0.2068
38.9149	−85.1145	25.0000	−0.2963	−0.9432	0.1503
17.2733	−73.5213	25.0000	−0.6271	−0.7767	0.0584
0.9046	−55.1578	25.0000	−0.8364	−0.5481	0.0042
−10.011	−33.064	25.0000	−0.9408	−0.3389	−0.0014
−16.6764	−9.2943	25.0000	−0.9702	−0.2425	0.0000
−22.667	14.668	25.0000	−0.9701	−0.2425	0.0000
−30.2156	38.1403	25.0000	−0.9048	−0.4241	−0.0384
−45.7867	56.918	25.0000	−0.5613	−0.8082	−0.1780
−68.5053	66.1778	25.0000	−0.1938	−0.9536	−0.2304
−93.0125	66.347	25.0000	0.2296	−0.9449	−0.2335
−111.837	51.6557	25.0000	0.8722	−0.4580	−0.1719
−118.1155	27.9078	25.0001	0.9754	−0.1096	−0.1911
−119.2883	3.2467	25.0000	0.9767	−0.0111	−0.2142
−119.473	−21.4523	25.0000	0.9756	−0.0094	−0.2195
−119.9058	−46.1475	25.0000	0.9762	−0.0253	−0.2154
−120.7568	−70.832	25.0000	0.9775	−0.0419	−0.2068

References

1. Jha BK, Kumar A (2003) Analysis of geometric errors associated with five-axis machining centre in improving the quality of cam profile. Int J Mach Tool Manu 43(6):629–636. doi:10.1016/S0890-6955(02)00268-7
2. Soichi I, Goh S, Kunitaka T (2014) 'Open-loop' tracking interferometer for machine tool volumetric error measurement—two-dimensional case. Precis Eng 38(3):666–672. doi:10.1016/j.precisioneng.2014.03.004
3. Xiang S, Yang J, Zhang Y (2014) Using a double ball bar to identify position-independent geometric errors on the rotary axes of five-axis machine tools. Int J Adv Manuf Technol 70(9):2071–2082. doi:10.1007/s00170-013-5432-9
4. Hong C, Ibaraki S, Oyama C (2012) Graphical presentation of error motions of rotary axes on a five-axis machine tool by static R-test with separating the influence of squareness errors of linear axes. Int J Mach Tool Manu 59(2):24–33. doi:10.1016/j.ijmachtools.2012.03.004
5. Matsushita T, Oki T, Matsubara A (2008) The accuracy of cone frustum machined by five-axis machine tool with tilting table. J Jpn Soc Precis Eng 74(6):632–636. doi:10.2493/jjspe.74.632
6. Weikert S (2004) R-test, a new device for accuracy measurements on five axis machine tools. CIRP Ann Manuf Technol 53(1):429–432. doi:10.1016/S0007-8506(07)60732-X
7. Mou WP, Song ZY, Guo ZP, Tang LM (2012) A machining test to reflect dynamic machining accuracy of five-axis machine tools. Adv Mater Res 622-623:414–419. doi:10.4028/www.scientific.net/AMR.622-623.414
8. Guan LW, Mo J, Fu M, Wang LP (2017) An improved positioning method for flank milling of s-shaped test piece. Int J Adv Manuf Technol:1–16. doi:10.1007/s00170-017-0180-x
9. Su Z, Wang L (2015) Latest development of a new standard for the testing of five-axis machine tools using an S-shaped test piece. Proc Inst Mech Eng B J Eng Manuf 229(7). doi:10.1177/0954405414560780
10. Wang W, Zhang XY, Mei X (2016) Research on the mechanism of free surface contour error caused by the stiffness of feed system of five-axis machine tools. J Mech Eng 52(21). doi:10.3901/JME.2016.21.146
11. Wang W, Jiang Z, Li Q, Tao W (2015) A new test part to identify performance of five-axis machine tool-part ii validation of s part. Int J Adv Manuf Technol 79(5):739–756. doi:10.1007/s00170-015-6869-9
12. Li DU, Zheng CZ, Bian ZY, Zhao XD, Wang W (2015) Research on reconstruction and optimization of the "S"shaped test piece. Modular Machine Tool & Automatic Manufacturing Technique. doi:10.13462/j.cnki.mmtamt.2015.04.002
13. Du L, Zhang X, Zhao S, Li J (2014) Research on five-axis cnc machining method of S shaped detection test piece. China Mech Eng 25(21):2907–2911. doi:10.3969/j.issn.1004-132X.2014.21.013
14. Du L, Zhang X, Wang W, Fu ZH, Shi RB (2014) Research on properties of "S" shaped test piece on synthesis dynamic accuracy detection of five-axis cnc machine tools. J Univ Electron Sci Technol China 43(4):629–635. doi:10.3969/j.issn.1001-0548.2014.04.028
15. Song Z, Cui Y (2010) S-shape detection test piece and a detection method for detecting the precision of the numerical control milling machine. US, US 20100004777 A1
16. Liang Q, Wang YZ, Hong Y, Zhen Y (2008) Cutting path planning for ruled surface impellers. Chin J Aeronaut 21(5):462–471. doi:10.1016/S1000-9361(08)60060-6
17. Chiou JCJ (2004) Accurate tool position for five-axis ruled surface machining by swept envelope approach. Comput Aided Des 36(10):967–974. doi:10.1016/j.cad.2003.10.001
18. Gong H, Cao LX, Liu J (2005) Improved positioning of cylindrical cutter for flank milling ruled surfaces. Comput Aided Des 37(12):1205–1213. doi:10.1016/j.cad.2004.11.006
19. Gong H, Fang FZ, Hu XT, Cao LX, Liu J (2010) Optimization of tool positions locally based on the bceltp for 5-axis machining of free-form surfaces. Comput Aided Des 42(6):558–570. doi:10.1016/j.cad.2010.02.006
20. Senatore J, Monies F, Redonnet JM, Rubio W (2007) Improved positioning for side milling of ruled surfaces: analysis of the rotation axis's influence on machining error. Int J Mach Tool Manu 47(6):934–945. doi:10.1016/j.ijmachtools.2006.07.008
21. Marciniak K (1991) Geometric modelling for numerically controlled machining. Oxford University Press, Oxford
22. Redonnet JM, Rubio W, Dessein G (1998) Side milling of ruled surfaces: optimum positioning of the milling cutter and calculation of interference. Int J Adv Manuf Technol 14(7):459–465. doi:10.1007/BF01351391
23. Rubio DW, Lagarrigue P, Dessein G, Pastor F (1998) Calculation of tool paths for a torus mill on free-form surfaces on five-axis machines with detection and elimination of interference. Int J Adv Manuf Technol 14(1):13–20. doi:10.1007/BF01179412
24. Anderson C (1988) Curves and surfaces in computer aided geometric design, by F. Yamaguchi. Curves and surfaces in computer aided geometric design. Springer-Verlag
25. Castillo R, Mendoza E, Comia J (2015) On minimum distance problem. Am Sci Res J Eng Technol Sci 11(1):84–95